

An Exact Solver for Satisfiability Modulo Counting with Probabilistic Circuits

Jinzhao Li, Nan Jiang, Yexiang Xue
Department of Computer Science, Purdue University
{li4255, jiang631, yexiang}@purdue.edu

Abstract

Satisfiability Modulo Counting (SMC) is a recently proposed general language to reason about problems integrating statistical and symbolic artificial intelligence. An SMC formula is an extended SAT formula in which the truth values of a few Boolean variables are determined by probabilistic inference. Existing approximate solvers optimize surrogate objectives, which lack formal guarantees. Current exact solvers directly integrate SAT solvers and probabilistic inference solvers resulting in slow performance because of many back-and-forth invocations of both solvers. We propose KOCO-SMC, an integrated exact SMC solver that efficiently tracks lower and upper bounds in the probabilistic inference process. It enhances computational efficiency by enabling early estimation of probabilistic inference using only partial variable assignments, whereas existing methods require full variable assignments. In the experiment, we compare KOCO-SMC with currently available approximate and exact SMC solvers on large-scale datasets and real-world applications. Our approach delivers high-quality solutions with high efficiency.

1 Introduction

Symbolic and statistical Artificial Intelligence (AI) are two foundations with distinct strengths and limitations. Symbolic AI, exemplified by SATisfiability (SAT) and constraint programming, excels in constraint satisfaction but cannot handle probability distributions. Statistical AI captures probabilistic uncertainty but does not guarantee to satisfy the symbolic constraints. Integrating symbolic and statistical AI remains an open field and has gained much research attention recently [18, 32, 33, 10, 40].

The recently proposed Satisfiability Modulo Counting (SMC) [17, 29] provides a general language to reason about problems integrating statistical and symbolic AI. Specifically, an SMC formula is an SAT formula in which the truth values of certain Boolean variables are determined through probabilistic inference, which assesses whether the marginal probability meets the given requirements. Solving SMC formulas poses significant challenges since they are NP^{PP} -complete [35].

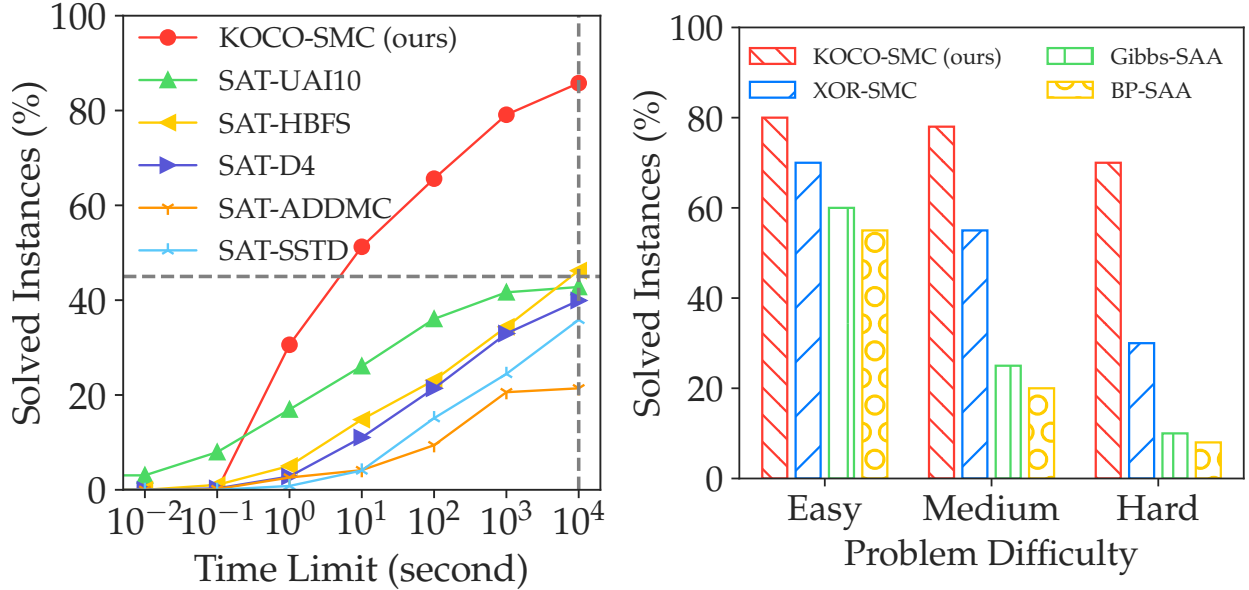


Figure 1: **(Left)** Compared to exact solvers, our KOCO-SMC solves 45% of SMC instances in the 10-second time limit, whereas baselines take 3 hours. **(Right)** Compared to approximate solvers, our KOCO-SMC solves 40% more instances in hard cases.

Take robust supply chain design as an example, shown in Figure 2, a manager needs to pick a route in the road map to ensure sufficient materials for good production, taking into account stochastic events such as natural disasters. This problem necessitates both symbolic reasoning to find a satisfiable route and statistical inference to ensure the roads are robust to stochastic natural disasters. The SMC formula is explained in Section 3.1. Slightly modified problems can be found in many real-world applications including vehicle routing [42], internet resilience [21], social influence maximization [22], energy security [1], etc.

Several approximate SMC solvers have been proposed [24, 29]. Approximate solvers based on Sample Average Approximation (SAA) [24] were the most widely implemented, which used sample mean to estimate the marginal probability. Another approximate solver, XOR-SMC [29], offers a constant approximation guarantee, by using the XOR-sampling to estimate the marginal probability. Yet the solution quality of approximate solvers lacks a formal guarantee. The solution could still violate a fraction of the constraints.

Current exact SMC solvers directly combine an SAT solver for satisfiability with a probabilistic inference solver for statistical inference. Specifically, the SAT solver first gives a feasible variable assignment for the Satisfiability part, which is then evaluated by a probabilistic inference solver. This method results in an excessive number of back-and-forth invocations between two solvers. Particularly for unsatisfiable problems, these exact SMC solvers enumerate all possible solutions before confirming unsatisfiability and thus are extremely slow. A motivating example is in Section 3.1.

We introduce KOCO-SMC, an exact and efficient SMC solver, mitigating the extreme slowness typically encountered in unsatisfiable SMC problems. KOCO-SMC saves time by detecting

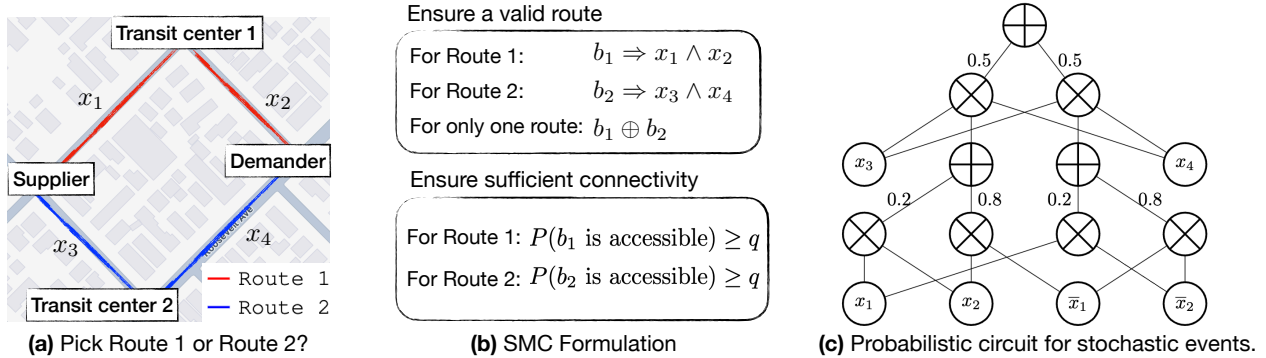


Figure 2: Formulation of the robust supply chain problem into SMC formula. **(a)** shows a road map containing 4 locations and the road between them. The connectivity of each road is denoted by a random variable x_i , where $x_i = \text{True}$ indicates the corresponding road is selected. **(b)** Model the supply routine planning as an SMC problem. **(c)** The probability of every connectivity situation, is represented as the Probabilistic Circuit. Each x_i or \bar{x}_i node denotes a leaf node that encodes a Bernoulli distribution. The symbols \oplus and \otimes represent the sum and product nodes respectively. The values next to the edges are weights for the sum nodes.

the conflict early with partial variable assignments. The proposed Upper Lower Watch (ULW) algorithm tracks the upper and lower bounds of probabilistic inference, when new variables are assigned. If these bounds violate the satisfaction condition, such as the probability’s upper bound drops below the minimum requirement, the conflicts are stored as learned clauses to avoid recurrence in future iterations.

In experiments, we evaluate all existing approximate and exact solvers on 1350 SMC problems—the largest dataset based on the UAI Competition benchmark. Figure 1 shows the comparison with state-of-the-art solvers. Compared with exact solvers, KOCO-SMC scales the best. Our KOCO-SMC solves 45% of instances within 10 seconds, whereas baseline methods require 3 hours. Given a 3-hour runtime, our approach can solve 85% of instances. Compared with those approximate solvers, KOCO-SMC reliably delivers higher quality solutions within the time limit. KOCO-SMC solves 40% more problems for hard SMC problems, whereas approximate solvers consistently produce infeasible solutions.

To summarize, our main contributions are: (1) We propose KOCO-SMC, an efficient exact solver for SMC problems, integrating probabilistic circuits for effective conflict detection. (2) Experiments on large-scale datasets illustrate KOCO-SMC’s superior performance compared to state-of-the-art approximate and exact baselines in both solution quality and time efficiency. (3) In the case study, we also demonstrate the process of formulating real-world problems into the SMC formula, and highlight the strong capability of our solver in addressing these problems.

2 Preliminaries

Satisfiability Modulo Counting (SMC) is a recently proposed extension of SAT [17, 29], which incorporates constraints that involve model counting. Recognizing the intrinsic connection be-

tween probabilistic inference and model counting, SMC adaptively captures the satisfiability problem in scenarios involving uncertainty.

Specifically, we use lower-case letters for random variables (i.e., x , y , z , and b) and use bold symbols (i.e., \mathbf{x} , \mathbf{y} , \mathbf{z} and \mathbf{b}) as vectors of Boolean variables, e.g., $\mathbf{x} = (x_1, \dots, x_n)$. Each variable x_i takes binary values in $\{\text{False}, \text{True}\}$. Given a formula ϕ for Boolean constraints and weighted functions $\{f_i\}_{i=1}^K$, and $\{g_i\}_{i=1}^K$ for the discrete probability distributions, the SMC problem is to determine if the following formula is satisfiable over random variables $\mathbf{x} = (x_1, x_2, \dots, x_n)$, $\mathbf{y}_i = (y_1, y_2, \dots, y_n)$, $\mathbf{z}_i = (z_1, z_2, \dots, z_n)$ and $\mathbf{b} = (b_1, b_2, \dots, b_L)$:

$$\phi(\mathbf{x}, \mathbf{b}), \text{ where } b_i \Leftrightarrow \sum_{\mathbf{y}_i} f_i(\mathbf{x}, \mathbf{y}_i) \geq q_i \quad (1)$$

$$\text{or } b_i \Leftrightarrow \sum_{\mathbf{y}_i} f_i(\mathbf{x}, \mathbf{y}_i) \geq \sum_{\mathbf{z}_i} g_i(\mathbf{x}, \mathbf{z}_i). \quad (2)$$

Each function f_i (or g_i) is an unnormalized discrete probability function over Boolean variables in \mathbf{x} and \mathbf{y}_i (respectively, \mathbf{x} and \mathbf{z}_i). The summation $\sum f_i$ and $\sum g_i$ compute the marginal probabilities, where \mathbf{y}_i and \mathbf{z}_i are latent variables and will be marginalized out. Thus, only \mathbf{x} and \mathbf{b} are decision variables. Each b_i is referred to as a *Probabilistic Predicate*, which is evaluated as true if and only if the inequality over the marginalized probability is satisfied. Each probabilistic constraint is in the form of either (1) the marginal or joint probability surpassing a given threshold q_i , or (2) one marginal joint probability being greater than another. Note that the biconditional “ \Leftrightarrow ” can be generalized to “ \Rightarrow ” or “ \Leftarrow ” and the “ \geq ” inequality case in the above definition can be generalized to “ $=$, $>$ ” cases and also the reversed direction inequality “ \leq , $<$ ” cases.

In summary, this SMC formulation provides a general language to reason about problems integrating symbolic and statistical constraints. Specifically, the symbolic constraint is characterized by a Boolean satisfiability formula ϕ . The statistical constraint is captured by constraints involving the weighted model counting term $\sum f_i$.

Probabilistic Circuits (PCs) are a broad category of probabilistic models known for enabling a variety of exact and efficient inferences [7, 6, 37, 38, 23, 9, 43, 36]. Formally, PC is a computational graph encoding a probability distribution $P(\mathbf{x})$ over a set of random variables \mathbf{x} . The graph is composed of leaf nodes, product nodes, and sum nodes. Each node v represents a probability distribution over certain random variables.

Figure 2(c) gives an example PC over four variables. A leaf node u encodes a tractable probability distribution $P_u(x_i)$ over a single random variable x_i , such as Gaussian or Bernoulli distributions. A product node u defines a factorized distribution $P_u(\mathbf{x}) = \prod_{v \in \text{ch}(u)} P_v(\mathbf{x})$ where $\text{ch}(u)$ denotes the children nodes of u . A sum node u represents a mixture distribution $P_u(\mathbf{x}) = \sum_{v \in \text{ch}(u)} w_v P_v(\mathbf{x})$, where w_v represent the normalization weights of child node v . The root node r in the graph has no parent node. A probabilistic circuit is a model of its root node distribution.

Probabilistic circuits with specific structural properties enable efficient probability inference, such as computing partition functions, marginal probabilities, and maximum a posteriori estimates, all of which scale polynomially with circuit size [3].

3 Methodology

3.1 Motivation

We use supply chain design as a motivating example to highlight the limitations of current exact SMC solvers. In Figure 2(a), the task is to deliver materials from suppliers to demanders on a road map. Various random events, such as natural disasters and car accidents, may affect road connectivity. The goal is to pick a route with a sufficient road connection probability.

Let x_i be each road segment in the map, for $i = 1, \dots, 4$. In the Boolean formula ϕ , $x_i = \text{True}$ represents the selection of road x_i . In the probabilistic constraint, $x_i = \text{True}$ indicates that road x_i is accessible. The stochasticity of random events is formulated as a joint probability distribution over all roads $P(x_1, x_2, x_3, x_4)$. The probability of x_1 and x_2 being well connected is the marginal probability $P(x_1, x_2 \text{ are accessible}) = \sum_{x_3, x_4} P(x_1 = x_2 = \text{True}, x_3, x_4)$. We formulate the route choice as the Boolean variables b_1 and b_2 , where $b_1 = \text{True}$ (and similarly $b_2 = \text{True}$) indicates the selection of route 1 (or route 2, respectively). The choice is picking either route 1 ($b_1 = \text{True}$) or route 2 ($b_2 = \text{True}$). Let $q \in [0, 1]$ be the minimum required probability of good connectivity along the route. The task can be formulated as an SMC instance:

$$\begin{aligned} \phi &= \underbrace{(b_1 \oplus b_2)}_{(a)} \wedge \underbrace{(b_1 \Rightarrow x_1 \wedge x_2)}_{(b)} \wedge \underbrace{(b_2 \Rightarrow x_3 \wedge x_4)}_{(c)}, \\ b_1 &\Leftrightarrow \underbrace{\sum_{x_3, x_4} P(x_1, x_2, x_3, x_4) \geq q}_{(e)}, \\ b_2 &\Leftrightarrow \underbrace{\sum_{x_1, x_2} P(x_1, x_2, x_3, x_4) \geq q}_{(f)} \end{aligned}$$

where \oplus is the logical “exclusive or” operator. In part (a), the constraint ensures that only one route is selected. In part (b), the clause indicates that: if route 1 is selected, both x_1 and x_2 must be assigned True. Part (c) applies a similar condition for route 2. In part (e), $\sum_{x_3, x_4} P(x_1, x_2, x_3, x_4)$ marginalizes out x_3 and x_4 , representing the probability of route 1’s condition under random natural disaster. Part (f) is analogous to part (e).

An existing exact SMC solver (like the SAT-* solver in our experiments) finds the route in the following manner. Assume $q = 0.5$, and use Figure 2(c) to model $P(x_1, x_2, x_3, x_4)$,

1. It first uses an SAT solver to solve the Boolean SAT problem $\phi(\mathbf{x}, \mathbf{b})$ and proposes a solution, e.g., $x_1 = x_2 = b_1 = \text{True}, x_3 = x_4 = b_2 = \text{False}$ (indicating route 1).
2. Then, it infers the marginal probability $\sum_{x_3, x_4} P(x_1 = x_2 = \text{True}, x_3, x_4) = 0.1 < q$, and find it violates the probabilistic constraint. See Figure 7 for calculation steps.
3. Since the assignment $x_1 = x_2 = \text{True}$ causes a conflict, we add clause $(\bar{x}_1 \vee \bar{x}_2)$ to formula ϕ to omit this assignment in the future. We then go back to step 1 and use the SAT solver for a new assignment.

The above process shows the SAT solver and probability inference are sequentially dependent. Each of them is waiting for the other to finish, which results in time waste. In the worst case, the SAT solver must enumerate all the solutions.

To address this issue, our KOCO-SMC immediately detects a conflict upon the partial assignment $x_1 = \text{True}$, saving time by avoiding further assignments to the remaining variables. Although x_2 is still unassigned, the highest possible probability value is below 0.5, i.e., $\max_{x_2} \sum_{x_3, x_4} P(x_1 = \text{True}, x_2, x_3, x_4) = 0.1 < 0.5$. This should trigger an immediate conflict instead of waiting for the SAT solver to assign x_2 . Therefore, KOCO-SMC can solve SMC problems more efficiently than existing exact SMC solver.

3.2 Main Pipeline of KOCO-SMC

This section presents the proposed KOCO-SMC approach for solving SMC problems both exactly and efficiently. KOCO-SMC follows the Conflict-Driven Clause Learning framework [41, 13], which comprises four key components: variable assignment, propagation, conflict clause learning, and backtracking. With the inclusion of probabilistic constraints in SMC problems, KOCO-SMC is further adapted to these steps. Algorithm 1 in the Appendix gives a broad overview.

Compilation. Initially, a knowledge compilation step transforms all probability distributions in probabilistic constraints probabilistic circuits with smooth and decomposable properties. This can be achieved by advanced tools [5, 8, 26]. An example is provided in Figure 2(c).

Variable Assignment. Pick one variable among the remaining free variables and assign it with a value $val \in \{\text{True}, \text{False}\}$. Practically, there are heuristics on the choice of variable and value to accelerate the whole process [12, 13, 19].

Propagation. This step is applied to simplify the whole formula given part of the assigned variables. For the Boolean constraints, the unit propagation is used to propagate new variable assignments across clauses. This process can create additional variable assignments or detect conflicts. For example, if we have the clauses $(x_1 \vee \neg x_2)$ and $(x_2 \vee x_3)$, and we assign $x_1 = \text{False}$, unit propagation would force $x_2 = \text{False}$, leading to further propagation $x_3 = \text{True}$. This significantly accelerates SAT solving. However, this procedure is specifically designed for Boolean clauses. How to incorporate probabilistic constraints into the propagation process, extract useful information from current variable assignments, and effectively detect conflicts remains an open problem. We propose the Upper-Lower Watch (ULW) approach, an efficient propagation method for probabilistic constraints that leverages the power of probabilistic circuits. By utilizing modern knowledge compilers, most common probability distributions can be compiled into tractable probabilistic circuits, making our approach broadly applicable.

Conflicts Clause Learning. A learned clause is a newly derived clause that adds to the current set of constraints after encountering a conflict. It enables the KOCO-SMC to remember and avoid the causes of previous conflicts, leading to much faster convergence.

Once a conflict is detected within a Boolean clause, there are existing techniques to add a learned clause to the original Boolean formula, avoiding the same conflict from occurring in the future. When a conflict arises in a probabilistic constraint, KOCO-SMC generates a learned conflict clause by negating the current variable assignments involved in the constraint and connecting them

with logical OR. For example, a conflict in $\sum_y P(x_1 = \text{True}, x_2 = \text{False}, y) > q$ will produce the clause $(\neg x_1 \vee x_2)$, preventing the assignment $x_1 = \text{True}, x_2 = \text{False}$ in future iterations.

Backtracking. This step is the process of undoing variable assignments when a conflict is detected, allowing the solver to explore alternative solutions.

3.3 Upper-Lower Watch for Conflict Detection in Probabilistic Constraints

The satisfaction or conflict of a probabilistic constraint is determined by the involved marginal probability. By maintaining a range of the marginal probability and refining it with each new variable assignment, we can detect satisfiability or conflict early when the range significantly deviates from the threshold. Let $\mathbf{x}_{\text{assigned}}$ be the assigned variables, \mathbf{x}_{rem} denote the unassigned variables, and \mathbf{y} be the marginalized-out latent variables. Determining the range of a marginal probability involves estimating the appropriate interval $[LB, UB]$, such that for all possible values assigned to \mathbf{x}_{rem} :

$$LB \leq \sum_{\mathbf{y}} P(\mathbf{x}_{\text{assigned}}, \mathbf{x}_{\text{rem}}, \mathbf{y}) \leq UB \quad (3)$$

The ‘‘upper bound’’ (UB) and ‘‘lower bound’’ (LB) serve as key constraints in our approach. The Upper-Lower Watch (ULW) algorithm monitors both values to track constraint violations. We show that computing sufficiently tight bounds can be reduced to a traversal of these circuits.

Each node v in the probabilistic circuit represents a distribution P_v over variables covered by its children. Our ULW algorithm associates each node with an upper bound $UB(v)$ and a lower bound $LB(v)$ for the marginal probability of P_v under the current assignment $\mathbf{x}_{\text{assigned}}$. Therefore, the $UB(r)$ and $LB(r)$ at the root node r are the upper and lower bounds of the whole probability.

To initialize or update the bounds, we traverse the probabilistic circuits in a bottom-up manner. The update rule for the leaf nodes is as follows:

- For a leaf node v over an assigned variable $x \in \mathbf{x}_{\text{assigned}}$, where variable x is assigned to val , update $UB(v) = LB(v) = P_v(x = val)$.
- For a leaf node v over an remaining variable $x \in \mathbf{x}_{\text{rem}}$, update $UB(v) = \max\{P_v(x = \text{True}), P_v(x = \text{False})\}$ and $LB(v) = \min\{P_v(x = \text{True}), P_v(x = \text{False})\}$.
- For a leaf node v over $y \in \mathbf{y}$ (the variable to be marginalized), update $UB(v) = LB(v) = 1$.

Let $ch(v)$ be the set of child nodes of v . Intermediate nodes, i.e., product nodes and sum nodes, can be updated by:

- For a product node p , update $UB(p) = \prod_{u \in ch(p)} UB(u)$, and $LB(p) = \prod_{u \in ch(p)} LB(u)$.
- For a sum node s , $UB(s) = \sum_{u \in ch(s)} w_u UB(u)$, and $LB(s) = \sum_{u \in ch(s)} w_u LB(u)$. Here w_u is the weight associated with each child node u .

During initialization, we traverse the entire probabilistic circuit once. When a new variable is assigned during the solving process, we only update from the affected leaf nodes to the root, ensuring efficiency. The correctness is guaranteed by the smoothness and decomposability properties of PCs. A former justification is provided in Lemma 1.

The bounds at the root node represent the bounds for the marginal probability in the constraint. Then we use the estimated bounds for conflict detection. If $LB(r)$ is greater than q in Eq. (1), the constraint is certainly satisfied. If $UB(r)$ is smaller than q , then the constraint is unsatisfiable. To avoid the same conflict, ULW put the negate of current variable assignments as a learned clause.

Lemma 1. *Let probabilistic circuit $P(\mathbf{x}, \mathbf{y})$ defined over Boolean variables $\mathbf{x} = (x_1, \dots, x_N)$ and $\mathbf{y} = (y_1, \dots, y_M)$. If it satisfies the smooth and decomposable property, then our ULW algorithm guarantees Eq. 3 holds. If all variables are assigned, the equality can be achieved for both LB and UB .*

Sketch of proof. The result is obtained by applying the theoretical properties of smooth, and decomposable probabilistic circuits to solve the marginal probability inference problem. Please refer to Appendix B for a detailed proof. \square

4 Related Works

Satisfiability Problems. Satisfiability (SAT) determines whether there exists an assignment of truth values to Boolean variables that makes the entire logical formula true. Numerous SAT solvers [12, 30, 13, 19] show great performance in various applications.

Conflict-Driven Clause Learning (CDCL) [41] is a modern SAT-solving algorithm that has been widely applied. The process begins by making decisions to assign values to variables and propagating the consequences of these assignments. If a conflict is encountered (i.e., a clause is unsatisfied), the solver performs conflict analysis to learn a new clause that prevents the same conflict in the future. The solver then backtracks to an earlier decision point, and the process continues. Through clause learning and backtracking, CDCL improves efficiency and increases the chances of finding a solution or proving unsatisfiability.

Probabilistic Inference and Model Counting. Probabilistic inference encompasses various tasks, such as calculating conditional probability, marginal probability, maximum a posteriori probability (MAP), and marginal MAP (MMAP). Each of them is essential in fields like machine learning, data analysis, and decision-making processes. Model counting calculates the number of satisfying assignments for a given logical formula, and is closely related to probabilistic inference. In discrete probabilistic models, computing probabilities can be translated to model counting.

Probabilistic Circuit. Probabilistic circuits with specific structural properties enable efficient probability inferences, scaling polynomially with circuit size. For example, partition functions and marginal probabilities are computed efficiently due to decomposability and smoothness, MAP requires determinism for maximization, and MMAP further requires Q-determinism [3].

The process of transforming a probability distribution into a probabilistic circuit with a specific structure is referred to as *knowledge compilation*. Several knowledge compilers, such as ACE [5],

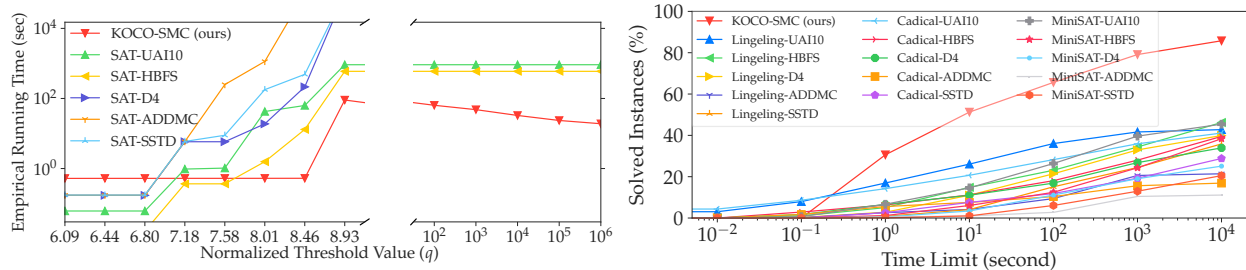


Figure 3: Comparing with exact solvers, KOCO-SMC solves 80% of SMC problems in 20 minutes while others solve 40% in 3 hours. **(Left)** The running time (x-axis) of experiments on a specific CNF and a Probabilistic Model with varying thresholds (y-axis). Our method typically requires significantly less time across most instances. Particularly when the threshold exceeds the critical point at which the SMC becomes UNSAT, our approach exhibits an improved performance. **(Right)** The percentage of instances solved in a given time limit.

C2D [8], and D4 [26], have been developed to convert discrete distributions into tractable PCs for various probabilistic inference tasks.

Specialized Satisfiability Modulo Counting. Stochastic Satisfiability (SSAT) [34] can encode SMC problems with a Boolean constraint and one single probabilistic constraint by integrating Boolean SAT with probabilistic quantifiers. Advances in SSAT solvers [27, 28, 14] have improved their efficiency, but these solvers remain limited to problems with a single probabilistic constraint and do not extend to general SMC formulations.

5 Experiments

We demonstrate KOCO-SMC’s high efficiency compared to baseline exact solvers (Figure 3) and the superiority in finding exact solutions compared to approximate solvers (Figure 5). To highlight the importance of ULW, we include an ablation study comparing performance with and without ULW (Figure 4). Additionally, we showcase its application to real-world problems (Figure 6).

5.1 Experiment Settings

SMC Problem Formulation For the experiment, we consider the satisfiability of the following SMC problem: $\phi(\mathbf{x}) \wedge \left(\sum_{\mathbf{y}} f(\mathbf{x}, \mathbf{y}) > q \right)$ where $\phi(\mathbf{x})$ is a Boolean formula in CNF, f is a (un-normalized) probability distribution, \mathbf{x} denotes the set of decision variables, \mathbf{y} represents variables to be marginalized, and $q \in \mathbb{R}$ is the threshold value. We exclude the variable \mathbf{b} from Equation 1 and fix the number of counting constraints to one in order to better control the properties of SMC problems. This allows us to gain clearer insights into the capabilities of our solver.

Dataset For f in the probabilistic constraints, we used the partition function-task benchmark that appears in the Uncertainty in Artificial Intelligence (UAI) Challenge from 2010 and 2022. 50 models over binary variables are kept. The remaining models can be grouped by 6 categories

Alchemy (1 model), *CSP* (3 models), *DBN* (6 models), *Grids* (2 models), *Promedas* (32 models), and *Segmentation* (6 models). For ϕ in the Boolean satisfiability, we randomly generated 9 different 3-coloring problems, in CNF, using CNFgen. The number of involved binary variables ranged from 75 to 675. The threshold value Q varies according to the task, and will be detailed in the respective sections.

Baselines We consider several approximate SMC solvers and exact SMC solvers. For the approximate solver, we include the Sampling Average Approximation (SAA) [24]-based method. Specifically, we use Lingeling [2] SAT solver to enumerate solutions and estimate $\sum_{\mathbf{y}} f(\mathbf{x}_f, \mathbf{y})$ by an average over samples, which enables approximate inference of marginal probabilities. We include Gibbs Sampler [39] (Gibbs-SAA) and Belief Propagation (BP-SAA) [15]. We also include XOR-SMC [29], an approximated solver specifically for SMC problems.

The baseline exact solver is composed of an exact SAT solver and probabilistic inference solvers. This approach first identifies a solution to the Boolean formula and then sequentially verifies it against the probabilistic constraints. For the Boolean SAT solver, we selected Lingeling [2] for its superior performance. For probabilistic inference, we selected top-performing solvers from the Uncertainty in Artificial Intelligence (UAI) Competitions. Due to limited access to these solvers, we chose the UAI2010 winning solver implemented in libDAI [31] (SAT-UAI10) and the solver based on the hybrid best-first branch-and-bound algorithm (SAT-HBFS) developed by Toulbar2 [4]. Although Toulbar2 was not the winner of the Partition Function or Marginal Probability tracks, it offers the necessary functionality and demonstrated strong performance in our tests. Due to the underlying connection between probabilistic inference and weighted model counting, we also include model counters from recent Model Counting competitions [16] from 2020 to 2023: d4 solver [26] (SAT-D4), ADDMC [11] (SAT-ADDMC), and SharpSAT-td [25] (SAT-SSTD).

Implementation of KOCO-SMC We applied ACE [5] as the knowledge compiler. The CDCL skeleton of KOCO-SMC is implemented on top of MiniSAT [13], for its easily extensible structure. For the ablation study, we include a version without ULW (KOCO-SMC without ULW).

5.2 Result Analysis

Comparison with Exact Solvers We study the performance of different exact SMC solvers facing SMC problems with different numbers of satisfying solutions. This is accomplished by changing the value of threshold Q and measuring the solving time. As the increase of Q , satisfying assignments become rare and finally unsatisfiable.

An illustrating result on a specific combination (*3-color-5x5.cnf* with *smokers_10.uai*) is shown in Figure 3(left). At low thresholds, all approaches quickly find a satisfying assignment; KOCO-SMC’s initial time is higher than average due to the pre-compilation of the probabilistic model. As the threshold rises, satisfying assignments become rare, leading to increased time costs. Notably, after the problem shifts from satisfiable to unsatisfiable, our methods’ (KOCO-SMC) time cost decreases, while others maintain high time consumption. This efficiency is due to our integrated ULW propagation, allowing early identification of unsatisfiability, while others have to enumerate all possible solutions before conclusion. In cases of extremely high thresholds, our method

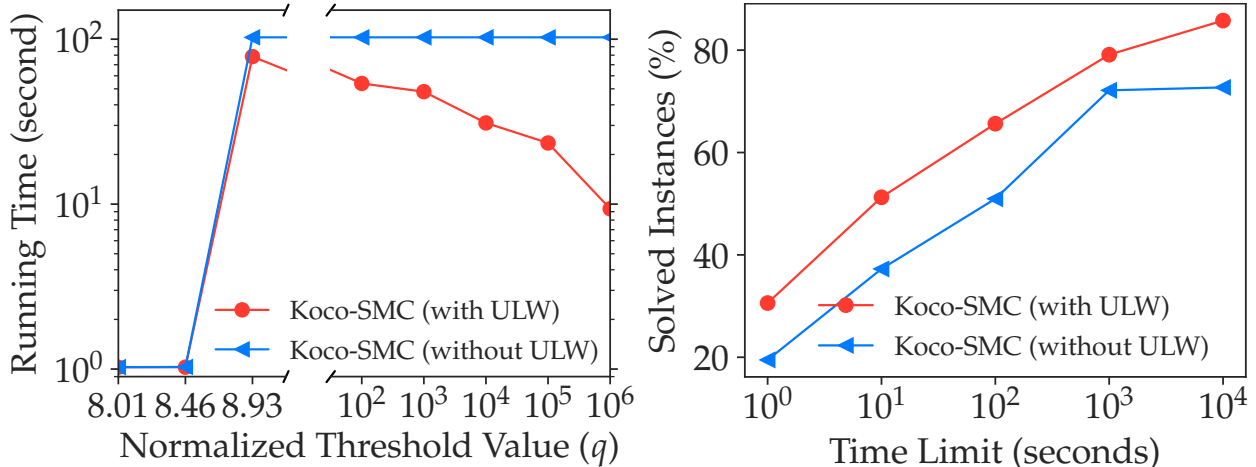


Figure 4: The ULW in KOCO-SMC is shown to be the key component in accelerating solving SMC formulas. **(Left)** The running time with varying thresholds. ULW propagation accelerates KOCO-SMC by 10 times compared with KOCO-SMC without ULW when the threshold reaches 10^6 . **(Right)** The percentage of instances solved in a given time limit. ULW helps KOCO-SMC to solve more instances within a given running time.

concludes unsatisfiability immediately.

The efficiency of KOCO-SMC is further demonstrated by evaluating the entire benchmark consisting of 1,350 different SMC instances. Figure 3(right) illustrates the relationship between the percentage of solved instances and running time. It is an extension of Figure 1(right), which includes MiniSAT (MINI-) and CaDiCal (CDC-) SAT solvers implemented in PySAT as the Boolean SAT oracle. KOCO-SMC shows the best performance among baselines.

Effectiveness of Upper-Lower Bound Watch Algorithm. In Figure 4(left), ULW propagation accelerates KOCO-SMC by 10 times compared with KOCO-SMC without ULW when the threshold reaches 10^6 . Figure 4(right) further demonstrates the contribution of ULW, where KOCO-SMC is 10 times faster than KOCO-SMC without UWL for SMC problems solvable around 10 minutes.

Comparison with Approximate Solvers Our approach is compared with baselines across a total of 9×50 combinations of benchmark CNF and probabilistic models. For each combination, we use the partition function of the probabilistic model multiplied by various scalars as the varying thresholds. The scalars range from 10^{-35} to 10^5 , as shown on the x-axis of Figure 5. Each approximate solver runs 5 times on each problem, and if one correct solution is found, the problem is considered “solved”. The portion of solved instances in 1 hour is shown in Figure 5.

As the threshold increases from 10^{-35} to 10^{-10} , most SMC formulas remain satisfiable, but the likelihood of finding a satisfying configuration decreases, causing a performance decline across all solvers. Between 10^{-5} and 10^5 , most formulas become unsatisfiable. Higher thresholds create more extreme conditions, enabling solvers to quickly detect unsatisfiability and improve performance. Overall, KOCO-SMC demonstrates its strong performance across varying threshold levels.

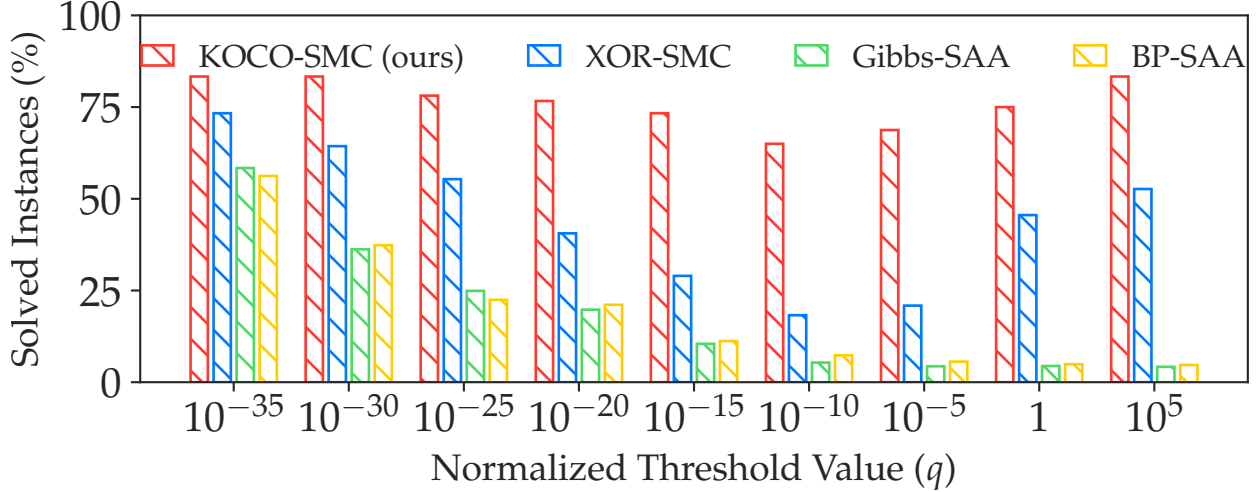


Figure 5: Compare KOCO-SMC with approximate solvers on solving SMC formulas across varying thresholds. KOCO-SMC consistently outperforms others, maintaining a higher percentage of solved formulas. As the threshold increases from 10^{-35} to 10^{-10} , the probability of discovering satisfying variable assignment decreases, leading to a drop in all solvers’ performance. From 10^{-5} to 10^5 , higher thresholds impose more extreme conditions, allowing solvers to quickly determine unsatisfiability, resulting in improved performance.

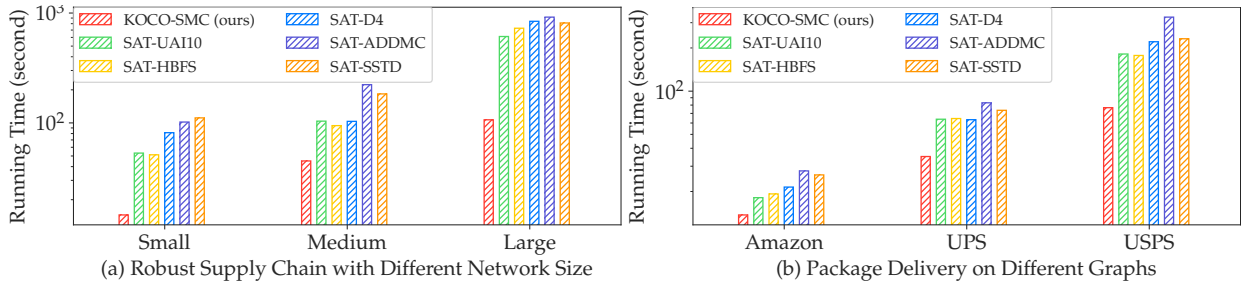


Figure 6: **(Left)** Running time of each method for identifying the best trading plan. All methods are tested on three real-world supply chain networks of different sizes. **(Right)** Running time for identifying the best delivery path. All methods are tested on three road maps of different sizes. Our KOCO-SMC finds all the best solutions significantly faster.

5.3 Case Studies

Application: Supply Chain Design The objective is to develop the best trading plan for each supplier in the supply chain network, ensuring that all trades have the highest success probability and satisfy the budget constraints. In the supply chain network, each supplier is represented as a node, which purchases raw materials from upstream nodes and sells products to downstream nodes. (1) To balance manufacturing safety and budget constraints, each node purchase raw materials from exactly two upstream suppliers and sells to exactly two downstream customers. (2) Trades may be disrupted by random events such as natural disasters, car accidents, or political issues. The trading plan must ensure a minimum probability of all trades succeeding, guaranteeing resilience against disruptions.

Let $x_e \in \{\text{True}, \text{False}\}$ represent the selection of a trade between nodes connected by edge e , where $x_e = \text{True}$ if the trade is selected. Combining the requirement (1) and (2), we have the SMC formulation: $\phi(\mathbf{x}_e) \wedge (\sum_{\mathbf{x}'} P(\mathbf{x}_e, \mathbf{x}') > q)$ where $\phi(\mathbf{x}_e)$ represents the budget constraints on the set of selected trades \mathbf{x}_e , q is the minimum requirement of successful probability, and $P(\cdot)$ is the probabilistic transportation model defined over all edges. The marginal probability $\sum_{\mathbf{x}'} P(\mathbf{x}_e, \mathbf{x}')$ is the probability that all selected trades are carried out successfully.

We use 4-layer supply chain networks from the bread supply chain dataset containing 44 nodes (Large) [45], where each layer represents a tier of suppliers. Additionally, we introduce synthetic networks with 20 nodes (Small) and 28 nodes (Medium) to improve illustration. To find the plan guaranteeing the highest success probability, we gradually increase the threshold q from 0 to 1 in increments of 1×10^{-2} , continuing until the threshold makes the SMC problem unsatisfiable.

The running time for finding the best plan is shown in Figure 6 (Left), and detailed settings are in Appendix C.5. Through a proper problem definition, KOCO-SMC demonstrates superior performance in finding the optimal plan.

Application: Package Delivery The task is to find a Hamiltonian path that covers major delivery locations while minimizing the chance of encountering heavy traffic [20]. The delivery locations and roads are modeled as nodes and edges, respectively. (1) The path must be Hamiltonian, passing through each node exactly once. (2) Each road segment has a probability of heavy traffic, depending on the time of travel, weather conditions, and road properties. The probability of encountering heavy traffic on any segmentation should be lower than a threshold.

Suppose there are N delivery locations indexed from 1 to N . Let $x_{i,j} \in \{\text{True}, \text{False}\}$, where $x_{i,j} = \text{True}$ if and only if the j -th location is visited in the i -th position of the path. Combining requirements (1) and (2), we derive the SMC formulation: $\phi(\mathbf{x}) \wedge (\sum_{\mathbf{e}} P(\mathbf{x}, \mathbf{e}) < q)$, where \mathbf{x} is the set of decision variables $x_{i,j}$, $i, j \in \{1, \dots, N\}$, \mathbf{e} is the set of latent environmental variables, and $P(\mathbf{x}, \mathbf{e})$ represents the probability of encountering heavy traffic given the path encoded by \mathbf{x} with the environmental conditions \mathbf{e} . The marginal probability $P(\mathbf{x}, \mathbf{e})$ is the exact likelihood of encountering heavy traffic. Finally, $q \in \mathbb{R}$ is the threshold value. Detailed settings are in Appendix C.6.

The graph structures used in our experiments are based on cropped regions from Google Maps. We consider three sets of delivery locations: 8 Amazon Lockers, 10 UPS Stores, and 6 USPS Stores. The three maps we examine are: Amazon Lockers only (Amazon), Amazon Lockers plus UPS Stores (UPS), and UPS graph with the addition of 6 USPS Stores (USPS). These graphs consist of 8, 18, and 24 nodes, respectively. The traffic condition probability is modeled by the Bayesian network from Los Angeles traffic data [44]. We gradually decrease the threshold q from 1 to 0 in increments of 10^{-2} , continuing until the threshold makes the SMC problem unsatisfiable. The running time for finding the best plan is shown in Figure 6 (Right). KOCO-SMC can efficiently discover an optimal plan with this proper SMC problem formulation.

6 Conclusion

We introduced KOCO-SMC for solving Satisfiability Modulo Counting problems exactly. Our method is distinct from existing approaches, which typically combine SAT solvers with model counters. Instead, we introduce an early conflict detection mechanism by comparing the upper and lower bounds of probabilistic inferences. Our proposed Upper Lower Watch algorithm enables efficient tracking of both bounds. Our experiments on large-scale datasets demonstrate that our KOCO-SMC achieves superior solution quality compared to approximate solvers and greatly outperforms existing exact solvers in terms of efficiency. The real-world application highlights the potential of solving practical problems.

References

- [1] R. Almeida, Qinru Shi, Jonathan M. Gomes-Selman, Xiaojian Wu, Yexiang Xue, H. Angarita, N. Barros, B. Forsberg, R. García-Villacorta, S. Hamilton, J. Melack, M. Montoya, Guillaume Perez, S. Sethi, C. Gomes, and A. Flecker. Reducing greenhouse gas emissions of amazon hydropower with strategic dam planning. *Nature Communications*, 10, 2019.
- [2] Armin Biere. Cadical, lingeling, plingeling, treengeling and yalsat entering the sat competition 2018. *Proceedings of SAT Competition*, 14:316–336, 2017.
- [3] YooJung Choi, Tal Friedman, and Guy Van den Broeck. Solving marginal MAP exactly by probabilistic circuit transformations. In *AISTATS*, volume 151 of *Proceedings of Machine Learning Research*, pages 10196–10208. PMLR, 2022.
- [4] Martin C Cooper, Simon De Givry, Martí Sánchez, Thomas Schiex, Matthias Zytnicki, and Tomas Werner. Soft arc consistency revisited. *Artificial Intelligence*, 174(7-8):449–478, 2010.
- [5] Adnan Darwiche and Pierre Marquis. A knowledge compilation map. *Journal of Artificial Intelligence Research*, 17:229–264, 2002.
- [6] Adnan Darwiche. Compiling knowledge into decomposable negation normal form. In *IJCAI*, volume 99, pages 284–289. Citeseer, 1999.
- [7] Adnan Darwiche. A logical approach to factoring belief networks. *KR*, 2:409–420, 2002.
- [8] Adnan Darwiche. New advances in compiling cnf to decomposable negation normal form. In *Proc. of ECAI*, pages 328–332. Citeseer, 2004.
- [9] Rina Dechter and Robert Mateescu. And/or search spaces for graphical models. *Artificial intelligence*, 171(2-3):73–106, 2007.
- [10] Louise Dennis, Marie Farrell, and Michael Fisher. Developing multi-agent systems with degrees of neuro-symbolic integration [a position paper]. *arXiv preprint arXiv:2305.11534*, 2023.

- [11] Jeffrey Dudek, Vu Phan, and Moshe Vardi. Addmc: weighted model counting with algebraic decision diagrams. In *Proceedings of the AAAI Conference on Artificial Intelligence*, volume 34, pages 1468–1476, 2020.
- [12] Jeffrey M. Dudek, Vu Phan, and Moshe Y. Vardi. ADDMC: weighted model counting with algebraic decision diagrams. In *AAAI*, pages 1468–1476. AAAI Press, 2020.
- [13] Niklas Eén and Niklas Sörensson. An extensible sat-solver. In *International conference on theory and applications of satisfiability testing*, pages 502–518. Springer, 2003.
- [14] Yu-Wei Fan and Jie-Hong R Jiang. Sharpssat: a witness-generating stochastic boolean satisfiability solver. In *Proceedings of the AAAI Conference on Artificial Intelligence*, volume 37, pages 3949–3958, 2023.
- [15] Ding Fan and Xue Yexiang. Contrastive divergence learning with chained belief propagation. In *International Conference on Probabilistic Graphical Models*, pages 161–172. PMLR, 2020.
- [16] Johannes K Fichte, Markus Hecher, and Florim Hamiti. The model counting competition 2020. *Journal of Experimental Algorithmics (JEA)*, 26:1–26, 2021.
- [17] Matthew Fredrikson and Somesh Jha. Satisfiability modulo counting: a new approach for analyzing privacy properties. In *CSL-LICS*, pages 42:1–42:10. ACM, 2014.
- [18] Eugene C. Freuder and Barry O’Sullivan, editors. *AAAI-23 Constraint Programming and Machine Learning Bridge Program*, 2023.
- [19] Youssef Hamadi, Said Jabbour, and Lakhdar Sais. Manysat: a parallel sat solver. *Journal on Satisfiability, Boolean Modeling and Computation*, 6(4):245–262, 2010.
- [20] Poo Kuan Hoong, Ian KT Tan, Ong Kok Chien, and Choo-Yee Ting. Road traffic prediction using bayesian networks. In *IET International Conference on Wireless Communications and Applications (ICWCA 2012)*, 2012.
- [21] Eitan Israeli and R Kevin Wood. Shortest-path network interdiction. *Networks: An International Journal*, 40(2):97–111, 2002.
- [22] David Kempe, Jon Kleinberg, and Éva Tardos. Influential nodes in a diffusion model for social networks. In *Automata, languages and programming*, pages 1127–1138. Springer, 2005.
- [23] Doga Kisa, Guy Van den Broeck, Arthur Choi, and Adnan Darwiche. Probabilistic sentential decision diagrams. In *Fourteenth International Conference on the Principles of Knowledge Representation and Reasoning*, 2014.
- [24] Anton J. Kleywegt, Alexander Shapiro, and Tito Homem-de-Mello. The sample average approximation method for stochastic discrete optimization. *SIAM J. Optim.*, 12(2):479–502, 2002.

- [25] Tuukka Korhonen and Matti Järvisalo. Sharpsat-td in model counting competitions 2021-2023. *arXiv preprint arXiv:2308.15819*, 2023.
- [26] Jean-Marie Lagniez and Pierre Marquis. An improved decision-dnnf compiler. In *IJCAI*, volume 17, pages 667–673, 2017.
- [27] Nian-Ze Lee, Yen-Shi Wang, and Jie-Hong R Jiang. Solving stochastic boolean satisfiability under random-exist quantification. In *IJCAI*, pages 688–694, 2017.
- [28] Nian-Ze Lee, Yen-Shi Wang, and Jie-Hong R Jiang. Solving exist-random quantified stochastic boolean satisfiability via clause selection. In *IJCAI*, pages 1339–1345, 2018.
- [29] Jinzhao Li, Nan Jiang, and Yexiang Xue. Solving satisfiability modulo counting for symbolic and statistical AI integration with provable guarantees. In *AAAI*, 2024.
- [30] Joao P Marques-Silva and Karem A Sakallah. Grasp: A search algorithm for propositional satisfiability. *IEEE Transactions on Computers*, 48(5):506–521, 1999.
- [31] Joris M. Mooij. libDAI: A free and open source C++ library for discrete approximate inference in graphical models. *Journal of Machine Learning Research*, 11:2169–2173, August 2010.
- [32] *Neuro-symbolic AI for Agent and Multi-Agent Systems (NeSyMAS) Workshop at AAMAS-23*, 2023.
- [33] *IBM Neuro-Symbolic AI Workshop 2023 – Unifying Statistical and Symbolic AI*, 2023.
- [34] Christos H Papadimitriou. Games against nature. *Journal of Computer and System Sciences*, 31(2):288–301, 1985.
- [35] James D. Park and Adnan Darwiche. Complexity results and approximation strategies for map explanations. *J. Artif. Int. Res.*, 2004.
- [36] Robert Peharz, Steven Lang, Antonio Vergari, Karl Stelzner, Alejandro Molina, Martin Trapp, Guy Van den Broeck, Kristian Kersting, and Zoubin Ghahramani. Einsum networks: Fast and scalable learning of tractable probabilistic circuits. In *ICML*, volume 119 of *Proceedings of Machine Learning Research*, pages 7563–7574. PMLR, 2020.
- [37] Hoifung Poon and Pedro M. Domingos. Sum-product networks: A new deep architecture. In *UAI*, pages 337–346. AUAI Press, 2011.
- [38] Tahrima Rahman, Prasanna V. Kothalkar, and Vibhav Gogate. Cutset networks: A simple, tractable, and scalable approach for improving the accuracy of chow-liu trees. In *ECML/PKDD (2)*, volume 8725 of *Lecture Notes in Computer Science*, pages 630–645. Springer, 2014.
- [39] Alexander Shapiro. Monte carlo sampling methods. *Handbooks in operations research and management science*, 10:353–425, 2003.

- [40] Amit P. Sheth, Kaushik Roy, and Manas Gaur. Neurosymbolic AI - why, what, and how. *CoRR*, abs/2305.00813, 2023.
- [41] JP Marques Silva and Karem A Sakallah. Grasp-a new search algorithm for satisfiability. In *Proceedings of International Conference on Computer Aided Design*, pages 220–227. IEEE, 1996.
- [42] Paolo Toth and Daniele Vigo. *The vehicle routing problem*. SIAM, 2002.
- [43] Antonio Vergari, Y Choi, Robert Peharz, and Guy Van den Broeck. Probabilistic circuits: Representations, inference, learning and applications. *AAAI Tutorial*, 2020.
- [44] Cody West. Los angeles traffic prediction bayesian network. https://github.com/cww2697/LA_Traffic_Bayesian_Net, 2020. Accessed: September 30, 2024.
- [45] Shiva Zokaee, Armin Jabbarzadeh, Behnam Fahimnia, and Seyed Jafar Sadjadi. Robust supply chain network design: an optimization model with real world application. *Annals of Operations Research*, 257:15–44, 2017.

A Extended Methodology

A.1 Probabilistic Inference through Probabilistic Circuits

The inference of probabilities from a probability circuit can be very efficient. Figure 7 shows a decomposable and smooth probability circuit. For $P(x_1 = x_3 = x_4 = \text{True}, x_2 = \text{False})$, set the value of nodes x_1 , x_3 , and x_4 to 1, and \bar{x}_1 to 0. Set nodes x_2 and \bar{x}_2 oppositely since $x_2 = \text{False}$. Evaluate the value at the root node as the probability, which is 0.1. This inference doesn't require any special property of the probabilistic circuit.

It is different for the marginal probability. We need the circuit to be decomposable and smooth to ensure efficacy. For $P(x_3 = x_4 = \text{True})$, set nodes x_3 and x_4 to 1 as they are assigned True. For the marginalized-out variables x_1 and x_2 , set all related nodes, e.g., x_1 and \bar{x}_1 , to 1. Evaluate the value at the root node, which should be 1.0.

A.2 KOCO-SMC Main Pipeline

Classical SAT solvers like MiniSAT [13] have achieved high performance in real-world applications. We implement our method based on their MiniSAT version 2.2.0¹. The decision and back-track steps are primarily from their implementation, but our propagation and conflict clause learning steps differ. The pseudocode is shown in Algorithm 1.

Pre-Compilation The tractable probabilistic circuits are constructed from the discrete probability distributions in the form of Bayesian networks or Markov Random Fields. The pipeline is introduced in [7] (Fig. 8) that compiles a distribution into a Boolean formula augmented with literal weights, and is further compiled into a tractable Boolean circuit—characterized by its determinism, decomposability, and smoothness. From this circuit, one derives a tractable probabilistic circuit. We use the knowledge compilation tool: ACE² using their default *compile* script.

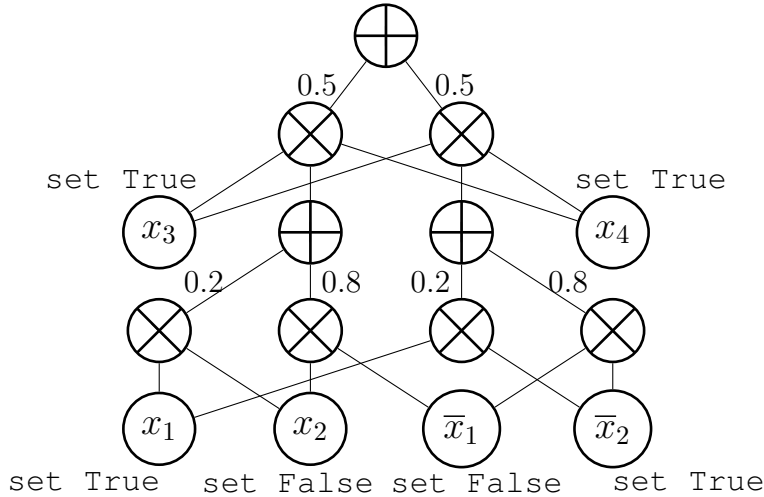
Decision To quickly identify a satisfying solution, the decision is made according to some decision heuristics. KOCO-SMC utilizes Variable State Independent Decaying Sum (VSIDS) [12] as the decision heuristic. Generally, each variable assignment is associated with a priority score. A higher score indicates a higher priority of being decided. During SMC-solving, once current variable assignments make the SMC problem unsatisfiable (also referred to as a *conflict*). The priority of those assignments will all decrease. All priority scores are then reduced by multiplying with a constant less than one. A variable's priority score is dynamically updated to reflect its recent involvement in conflicts.

Propagation The detailed implementation of propagation involving probabilistic constraints is shown in Algorithm 2, which corresponds to lines 4-8 of the Algorithm 1 in the main text. The explanation is as follows.

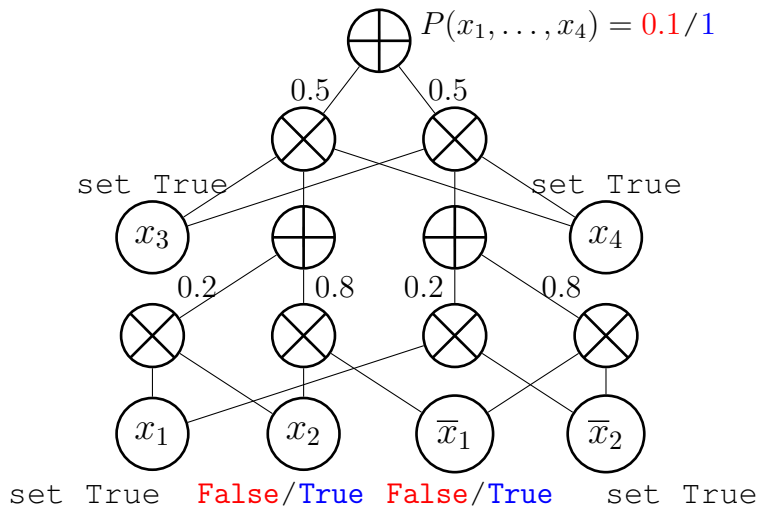
¹MiniSAT: <https://github.com/niklasso/minisat>

²ACE: <http://reasoning.cs.ucla.edu/ace>

$$P(x_1 = x_3 = x_4 = \text{True}, x_2 = \text{False}) = 0.1$$



(a) compute probability $P(x_1 = x_3 = x_4 = \text{True}, x_2 = \text{False})$



(b) compute marginal probability $P(x_3 = x_4 = \text{True})$.

Figure 7: To infer the probability $P(x_1 = x_3 = x_4 = \text{True}, x_2 = \text{False})$, set the value of nodes x_1 , x_3 , and x_4 to 1, and \bar{x}_1 to 0. Set values for x_2 and \bar{x}_2 oppositely since $x_2 = \text{False}$. The value assignment is shown in red, and the circuit evaluates to the probability 0.1. Similarly, to infer the marginal probability $P(x_3 = x_4 = \text{True})$, set nodes x_3 and x_4 to 1. For the marginalized-out variables x_1 and x_2 , set all related nodes to 1. The value assignment is shown in blue, and the circuit evaluates to the marginal probability 1.0.

Pick one new variable assignment (“new” refers to “hasn’t been propagated”): variable x assigned with value $val \in \{\text{True}, \text{False}\}$. The variable x is associated with a *watcher list*, denoted

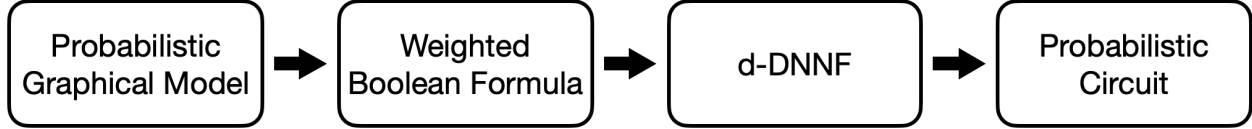


Figure 8: The process of constructing probabilistic circuits from probabilistic graphical models by ACE.

by $watcher(x)$, where each element is either a Boolean clause or a probabilistic constraint involving x . Once x is assigned with a value, only elements in $watcher(x)$ should verify its satisfiability under the current variable assignment. This mechanism is invented by [13]. It can avoid examining all constraints involving x and can improve efficacy, especially in problems with lots of constraints.

Consider a Boolean clause or probabilistic constraint C in $watcher(x)$. If C is a Boolean clause, we simply run the unit propagation. Otherwise, for each probabilistic circuit c_r in C , update the upper and lower bounds of each marginal probability encoded by c_r with current variable assignments. For example, a probabilistic constraint in the form of $b \Leftrightarrow \sum_y P(x, y) > Q$ contains one circuit encoding $P(x, y)$, we update the upper and lower bounds of $\sum_y P(x, y)$ with the current assignment of x . The detailed updating rule is specified in Section 3.3 of the main text. Then we can check the satisfiability with updated bounds, e.g., comparing the bounds of $\sum_y P(x, y)$ with threshold Q in the abovementioned example. If the comparison produces a conflict, e.g., the upper bound of $\sum_y P(x, y)$ is already below Q , then Algorithm 2 returns a conflict with the reference to current constraint as the reason (specified in line 10-11). Otherwise, we pick a new unassigned variable to watch, i.e., put the current constraint to the watcher list of another variable. Noted that we don't explicitly "remove" a satisfied probabilistic constraint as in MiniSAT to simplify the backtracking.

Conflict Clause Learning The clause learning step in line 13 of Algorithm 1 can be explained using the following example. Suppose the conflict is caused by a probabilistic constraint C , and the assigned variables in C are $x_1 = True$ and $x_2 = False$. Then the cause of conflict can be seen as $(\bar{x}_1 \vee x_2)$ (corresponds to line 2), which is exactly a Boolean clause in a CNF formula. Then we can utilize an experimentally effective method for Boolean SAT problems based on the First Unique Implication Point heuristic. We will not give a detailed definition here, please refer to [13] for detailed implementation.

Algorithm 1 Solving Satisfiability Modulo Counting Exactly with Probabilistic Circuits.

Input: Boolean Formula ϕ , Probabilistic Constraints $\{C_i\}_{i=1}^K$.

Output: Satisfiability and variable assignment.

```
1: Knowledge compilation ( $\{C_i\}_{i=1}^K$ ) ▷ preparation
2: loop
3:   Decide to assign variable  $x$  to  $val \in \{\text{True}, \text{False}\}$ . ▷ decision
4:   for each probabilistic constraint  $C$  in  $\{C_i\}_{i=1}^K$  do. ▷ propagation
5:     Update bounds of each circuit in  $C$  with  $v = val$ .
6:     Detect conflict by comparing bounds.
7:   for each Boolean clause  $C'$  in  $\phi$  do
8:     Propagate  $x = val$  to Boolean clause  $C'$ .
9:   if no conflict detected then
10:    if all variables assigned then
11:      return SAT, Variable assignments
12:    else
13:      Propose a learned clause  $C_l$ . ▷ clause learning
14:       $\phi \leftarrow \phi \cup \{C_l\}$ 
15:      if no variable assigned then
16:        return UNSAT, no assignment
17:      else
18:        undoing assignments until the reason no longer holds. ▷ Backtrack
```

B Proof of Lemma 1

Assumption 1 (Smooth and Decomposable [3]). *A smooth probabilistic circuit when all children of every sum node share identical sets of variables; A probabilistic circuit is decomposable if the children of every product node have disjoint sets of variables; Smoothness and decomposability enable tractable computation of any marginal probability query.*

Definition 1. *Denote assigned variables in \mathbf{x} as \mathbf{x}_e and those not assigned as \mathbf{x}_h . The exact upper and lower bounds of the marginal probability with the partial variable assignment are $\max_{\mathbf{x}_h} \sum_{\mathbf{y}} P(\mathbf{x}_e, \mathbf{x}_h, \mathbf{y})$ and $\min_{\mathbf{x}_h} \sum_{\mathbf{y}} P(\mathbf{x}_e, \mathbf{x}_h, \mathbf{y})$.*

Proof. Intuitively, to prove that $UB \geq \max_{\mathbf{x}_h} \sum_{\mathbf{y}} P(\mathbf{x}_e, \mathbf{x}_h, \mathbf{y})$ and $LB \leq \min_{\mathbf{x}_h} \sum_{\mathbf{y}} P(\mathbf{x}_e, \mathbf{x}_h, \mathbf{y})$, we need to relate the updating scheme with the marginal probability inference. Using the update steps for UB as an example, suppose $\mathbf{x}_h^* = \arg \max_{\mathbf{x}_h} \sum_{\mathbf{y}} P(\mathbf{x}_e, \mathbf{x}_h, \mathbf{y})$ maximizes the marginal probability. According to our ULW algorithm,

- Consider a leaf node v over a single variable $x \in \mathbf{x}_e$, then $UB(v) = P_v(x)$. If v is a leaf node over a variable $x \in \mathbf{x}_h$, then $UB(v) = \max_x P_v(x) \geq P_v(x^*)$. If v is a leaf node over a variable $y \in \mathbf{y}$, then $UB(v) = \sum_y P_v(y) = 1$.

Algorithm 2 Propagation

Input: The set of new assignments S .

Output: Conflict detection result

```
1: while  $S$  not empty do
2:    $x, val \leftarrow S.pop()$  ▷ variable  $x$  is assigned with value  $val$ 
3:   for  $C \in watcher(x)$  do
4:     if  $C$  is a Boolean clause then
5:       Unit propagation
6:     if  $C$  is a probabilistic constraint then
7:       for  $c_r \in circuits(C)$  do
8:         update bounds of the marginal probability
9:         encoded by  $c_r$ 
10:    if  $C$  is unsatisfied then
11:      return CONFLICT,  $C$ 
12:    if  $C$  has another unassigned variable  $x'$  then
13:      Add  $C$  to  $watcher(x')$ 
14:      Remove  $C$  from  $watcher(x)$ 
15:  return NO CONFLICT, No conflict reason
```

From this, we conclude that our approach overestimates the values of leaf nodes corresponding to \mathbf{x}_h , while other nodes remain unchanged in the marginal probability computation. Once all variables are assigned, the leaf nodes are evaluated exactly as in marginal probability inference.

- Suppose v is a product node. An example is shown in Figure 9. Without loss of generality, assume v has 2 child nodes: v_1 and v_2 that encodes $P_{v_1}(\mathbf{x}_e^{(1)}, \mathbf{x}_h^{(1)}, \mathbf{y}^{(1)})$ and $P_{v_2}(\mathbf{x}_e^{(2)}, \mathbf{x}_h^{(2)}, \mathbf{y}^{(2)})$ respectively. The decomposability property indicates that all its child nodes share no common variable. So the maximum of the product can be computed as the product of the maximum. Specifically, we have

$$\begin{aligned} UB(v) &= UB(v_1) \cdot UB(v_2) \max_{\mathbf{x}_h^{(1)}} \sum_{\mathbf{y}^{(1)}} P_{v_1}(\mathbf{x}_e^{(1)}, \mathbf{x}_h^{(1)}, \mathbf{y}^{(1)}) \cdot \max_{\mathbf{x}_h^{(2)}} \sum_{\mathbf{y}^{(2)}} P_{v_2}(\mathbf{x}_e^{(2)}, \mathbf{x}_h^{(2)}, \mathbf{y}^{(2)}) \\ &= \max_{\mathbf{x}'_h} \sum_{\mathbf{y}^{(1)}} \sum_{\mathbf{y}^{(2)}} P_{v_1}(\mathbf{x}_e^{(1)}, \mathbf{x}_h^{(1)}, \mathbf{y}^{(1)}) P_{v_2}(\mathbf{x}_e^{(2)}, \mathbf{x}_h^{(2)}, \mathbf{y}^{(2)}) \\ &= \max_{\mathbf{x}'_h} \sum_{\mathbf{y}'} P_{v_1}(\mathbf{x}_e^{(1)}, \mathbf{x}_h^{(1)}, \mathbf{y}^{(1)}) P_{v_2}(\mathbf{x}_e^{(2)}, \mathbf{x}_h^{(2)}, \mathbf{y}^{(2)}) \\ &= \max_{\mathbf{x}'_h} \sum_{\mathbf{y}'} P_v(\mathbf{x}'_e, \mathbf{x}'_h, \mathbf{y}') \end{aligned}$$

- Suppose v is a sum node. Note that the probabilistic circuit should be smooth. Without loss of generality, assume v has 2 child nodes v_1 and v_2 that encodes P_{v_1} and P_{v_2} , and their weights are

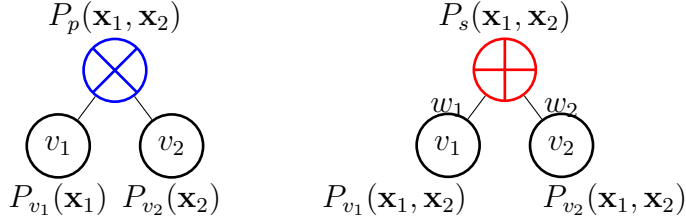


Figure 9: **(Left)** Example of a decomposable product node (colored blue). Denote the product node as p , and it has two children v_1 and v_2 . Child nodes encode $P_{v_1}(\mathbf{x}_1)$ and $P_{v_2}(\mathbf{x}_2)$ respectively and the product node encodes $P_p(\mathbf{x}_1, \mathbf{x}_2) = P_{v_1}(\mathbf{x}_1)P_{v_2}(\mathbf{x}_2)$. Decomposability ensures \mathbf{x}_1 and \mathbf{x}_2 are disjoint. **(Right)** Example of a smooth sum node (colored red). Denote the sum node as s , and it has two children v_1 and v_2 with weights w_1 and w_2 . Child nodes encode $P_{v_1}(\mathbf{x}_1, \mathbf{x}_2)$ and $P_{v_2}(\mathbf{x}_1, \mathbf{x}_2)$ respectively and the sum node encodes $P_s(\mathbf{x}_1, \mathbf{x}_2) = w_1P_{v_1}(\mathbf{x}_1, \mathbf{x}_2) + w_2P_{v_2}(\mathbf{x}_1, \mathbf{x}_2)$. Smoothness ensures all nodes encode probabilities over the same set of variables.

w_1 and w_2 respectively. The smoothness ensures that all its child nodes have the same scope of variables.

$$\begin{aligned}
 UB(v) &= w_1UB(v_1) + w_2UB(v_2) \\
 &\geq \max_{\mathbf{x}'_h} \left(\sum_{\mathbf{y}'} w_1 P_{v_1}(\mathbf{x}'_e, \mathbf{x}'_h, \mathbf{y}') \right) + \max_{\mathbf{x}'_h} \left(\sum_{\mathbf{y}'} w_2 P_{v_2}(\mathbf{x}'_e, \mathbf{x}'_h, \mathbf{y}') \right) \\
 &= \max_{\mathbf{x}'_h} \sum_{\mathbf{y}'} P_v(\mathbf{x}'_e, \mathbf{x}'_h, \mathbf{y}')
 \end{aligned}$$

Using the calculation defined above, we can recursively calculate $UB(r)$ for the root node r . Since r encodes $P(\mathbf{x}_e, \mathbf{x}_h, \mathbf{y})$, the strict upper bound is calculated. Similar steps and proof can be generalized to the lower bound. Our proposed ULW follows the calculation steps shown above. The calculation requires only one traversal of the probabilistic circuit. \square

C Experiment Setting

C.1 KOCO-SMC Implementation

In addition, frequent variable assignments can be empirically slow due to the need for constant bound updates. Inspired by the Two-Literal Watch technique [30], where the propagation reaches a Boolean clause only when two specific literals are newly assigned—regardless of the number of literals in the clause—we apply a similar strategy to probabilistic constraints. We define two watched variables for each probabilistic constraint: one decision variable and the probabilistic predicate. For instance, in $b_1 \Leftrightarrow \sum_{y_1, y_2} P(x_1, x_2, y_1, y_2)$, we designate b_1 and either x_1 or x_2 as the watched variables. The upper and lower bounds of $\sum_{y_1, y_2} P(x_1, x_2, y_1, y_2)$ are updated only when one of the watched variables is assigned, and this process continues until no unassigned variables remain.

C.2 Baselines

Gibbs-SAA and BP-SAA are approximate SMC solvers based on Sample Average Approximation. The marginal probability in the form of $\sum_y P(x, y)$ is approximated by samples from a sampler. More specifically, use the sampler to generate a set of samples $\{(x, y^{(i)})\}$ according to the distribution proportional to the $P(x, y)$. Then the estimation of the marginal probability is the sample average $\frac{1}{N} \sum_{y^{(i)}} P(x, y^{(i)})$ multiplied by the number of possible configurations of y , for binary variables of length n , there are 2^n possible configurations. We used Gibbs Sampler (Gibbs-SAA) and Belief Propagation (BP-SAA) implemented by [15] as the sampler. However, the sampling is only an efficient probability inference method, it still requires determining x forehead, thus we use MiniSAT to enumerate solutions of $\phi(x)$.

Given a time limit of 1 hour, we set the number of samples to 10000 and the number of Gibbs burn-in steps to 40. For each SMC problem in the benchmark dataset, we run Gibbs-SAA 5 times and the problem is considered "solved" as one of those runs produces a correct result. The percentage of solved SMCs is shown in Figure 5.

XOR-SMC is an approximate solver from [29]. We set the parameter T (controlling the probability of a satisfying solution, a higher T gives a better performance but longer run time) to 3, and incrementally increase the number of XOR constraints from 0 to either timeout or failed, by doing this we can find the most probable satisfying solution. Similar to SAA based approaches, we also run XOR-SMC 5 times.

Lingeling-LibDAI and Lingeling-Toulbar2 are the integration of an SAT solver, Lingeling [2], with the winning probabilistic inference solver of UAI Approximate Inference Challenge. The procedure is first run Lingeling to produce one solution satisfying the Boolean formula in an SMC problem, then use the inference solver to calculate the marginal probability given those assignments. If the marginal probability exceeds the threshold, the solution is reported and exits. Otherwise, let the SAT solver produce another different solution and redo the procedure until all solutions have been enumerated. The repetitive file I/O and solvers' initialization time throughout the process have been pruned for a fair comparison. Lingeling-LibDAI uses the public inference solver implemented by LibDAI [31] available on github³. Lingeling-Toulbar2 uses another inference solver Toulbar2 [4] which uses a hybrid best-first branch-and-bound algorithm (HBFS) to solve marginal probability. We use the public implementation of Toulbar2⁴ for PR task with their default parameters.

Lingeling-D4, Lingeling-ADDMC, and Lingeling-SSTD are integrations of the Lingeling SAT solver with the weighted model counting solver in the Model Counting Competition from 2020-2023. SAT-D4⁵ uses d4 solver based on knowledge compilation. SAT-ADDMC uses the public

³LibDAI: <https://github.com/dbtsai/libDAI/>

⁴Toulbar2: <https://toulbar2.github.io/toulbar2/>

⁵d4: <https://github.com/crillab/d4>

implementation of ADDMC solver⁶. SAT-SSTD uses SharpSAT-TD⁷ as the model counter.

C.3 Hyper-Parameter Settings

In all experiments, we use the public version of Lingeling implemented in PySAT⁸ with their default parameter. The time limit for all approximate solvers (Gibbs-SAA, XOR-SMC) is set to 1 hour per SMC problem. The time limit for all exact solvers is 3 hours. All experiments are executed on two 64-core AMD Epyc 7662 Rome processors with 16 GB of memory.

C.4 Dataset Specification

All SMC problems in this study are in the form of $\phi(\mathbf{x}_\phi, \mathbf{x}_f) \wedge \left(\sum_{\mathbf{y}} f(\mathbf{x}_f, \mathbf{y}) > q \right)$ where $\phi(\mathbf{x}_\phi, \mathbf{x}_f)$ is a CNF Boolean formula, f is a (unnormalized) probability distribution. \mathbf{x}_ϕ are variables appear only in ϕ , \mathbf{x}_f are random variables shared by ϕ and f , and \mathbf{y} are variables to be marginalized.

Boolean Formula All $\phi(\mathbf{x}_\phi, \mathbf{x}_f)$ represent 3-coloring problems for graphs, which is to find an assignment of colors to the nodes of the graph such that no two adjacent nodes have the same color, and at most 3 colors are used to complete color the graph. Then each node in the graph corresponds to 3 random variables, says x_1 x_2 and x_3 , that $x_1 = True$ iff. this node is colored with the first color. We consider only grid graphs of size k by k , resulting in $k \times k \times 3$ variables.

Those Boolean formulas are generated by CNFgen⁹ using the command

```
./cnfgen kcolor 3 grid k k -T shuffle
```

where the graph size k is set to 5, 10, and 15. For each grid graph, we shuffle the variable names randomly and keep 3 of them.

Probability Distribution We use probabilistic graphical models from the UAI competition 2010-2022¹⁰ including Markov random fields and Bayesian networks for the probabilistic constraints. Specifically, we pick the data for PR inference task, which includes 8 categories: Alchemy (2 models), CSP (3), DBN (6), Grids (8), ObjectDetection (79), Pedigree (3), Promedas (33), and Segmentation (6). The models with non-Boolean variables are removed, resulting in the remaining 50 models: *Alchemy* (1 model), *CSP* (3), *DBN* (6), *Grids* (2), *Promedas* (32), and *Segmentation* (6). All distributions are in the UAI file format. Since model counters d4, ADDMC, and SharpSAT-TD only accept weight CNF format in the model counting competition, we use bn2cnf¹¹ to convert data.

⁶ADDMC: <https://github.com/vardigroup/ADDMC>

⁷SharpSAT-TD: <https://github.com/Laakeri/sharpsat-td>

⁸PySAT: <https://pysathq.github.io/>

⁹CNFgen: <https://massimolauria.net/cnfgen/>

¹⁰UAI2022: <https://uaicompetition.github.io/uci-2022/>

¹¹bn2cnf: <https://www.cril.univ-artois.fr/KC/bn2cnf.html>

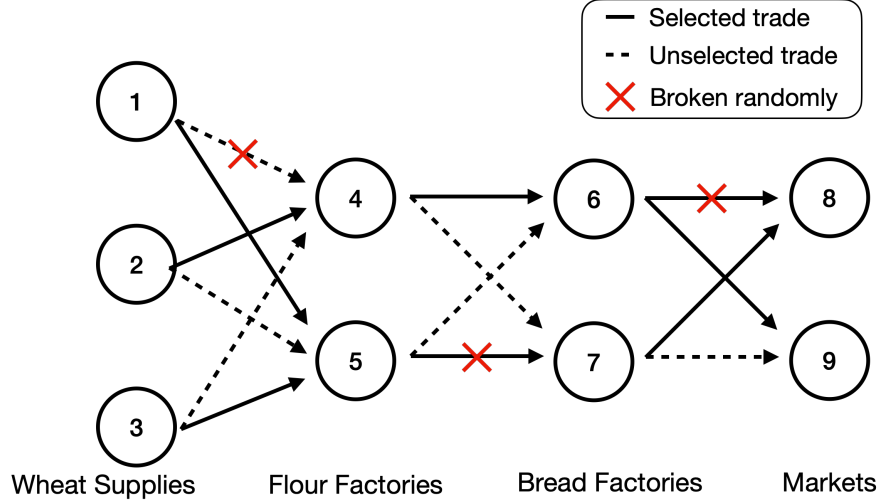


Figure 10: An example supply chain network. Edges with the red cross sign mean they are broken due to natural disasters.

Boolean Variables Classification We pick random variables from ϕ and f as shared variables uniformly at random. The number of shared variables between ϕ and f (denoted as x_f) is determined as the lesser of either half the number of random variables in f or the total number of random variables in ϕ , i.e., the count of variables in x_f will not surpass either half the total number of variables in f or the entire count of variables in ϕ .

C.5 Application: Supply Chain Design

For the experiment on real-world supply chain network data, we refer to a 4-layer supply chain network collected from real-world data [45]. This network consists of 4 layers of nodes, representing suppliers, with each layer containing 9, 7, 9, and 19 nodes, respectively. Adjacent layers are fully connected, meaning each node can trade with any node in the adjacent layers (nearest upstream suppliers and downstream demanders). An example is shown in Figure 10. Each edge between two nodes represents a trade between them, and the selection of trades can be encoded as a binary vector $x \in \{0, 1\}^M$, where M is the number of edges. Here, $x[i] = 1$ indicates that the i -th edge (trade) is selected.

The original problem does not account for stochastic disasters, so we generated a random Bayesian Network (BN) over all edges to model such events. For example, $P(x_1 = \text{True}, x_2 = \text{False})$ represents the probability that trade 1 is successful while trade 2 fails. Each BN node can have at most 5 parents, and the number of BN edges is approximately half of the maximum possible number. The generated BN is included in the code repository.

Due to budget constraints, each node is assumed to receive raw materials from exactly 2 upstream suppliers and sells its product to exactly 2 downstream demanders. We want the probability that all trades are successfully conducted to be above a certain threshold, even in the face of random

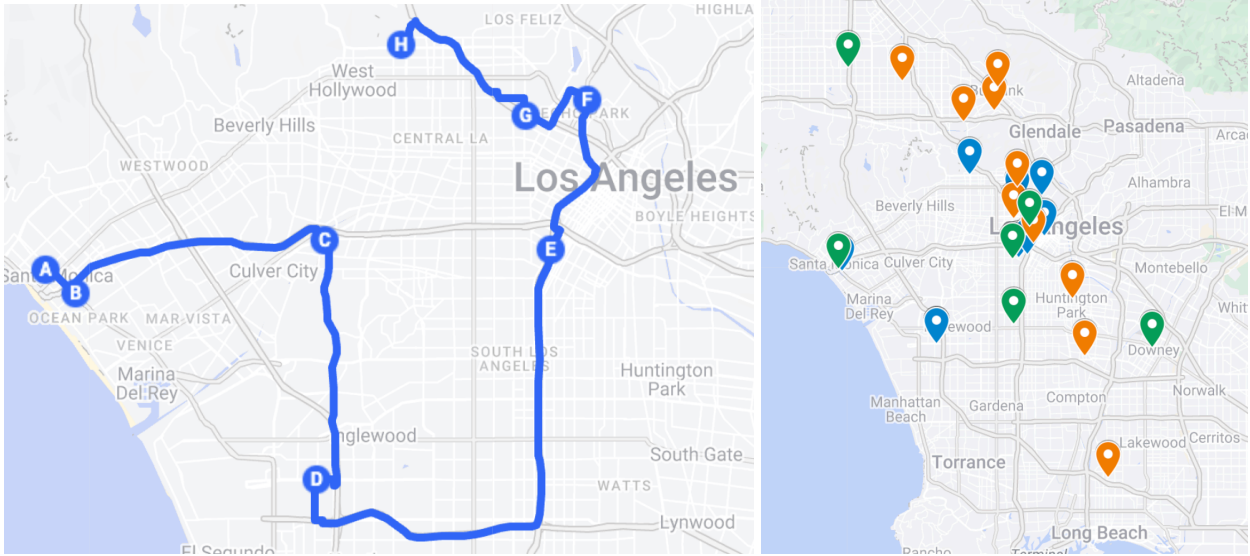


Figure 11: **(Left)** Example Hamiltonian delivery path covering major Amazon’s lockers in Los Angeles. **(Right)** delivery locations included in experiments. Blue points are Amazon lockers, orange points are UPS stores, and green points are USPS stores.

events such as natural disasters. We have the formulation:

$$\phi(\mathbf{x}, \mathbf{x}') \wedge \left(\sum_{\mathbf{x}'} P(\mathbf{x}, \mathbf{x}') > q \right)$$

where $\phi(\mathbf{x}, \mathbf{x}')$ represents the plan of executing trades \mathbf{x} while discarding \mathbf{x}' to satisfy the budget constraints. The marginal probability $\sum_{\mathbf{x}'} P(\mathbf{x}, \mathbf{x}')$ is exactly the probability that all selected trades are carried out successfully. To find the optimal plan, we gradually increase the threshold Q from 0 to 1 in increments of 1×10^{-3} , continuing until the threshold makes the SMC problem infeasible. The last feasible solution is referred to as the best plan.

We test all exact SMC solvers on 3 supply chain networks, including a small [5, 5, 5, 5], a medium [7, 7, 7, 7], and a large network [9, 7, 9, 19]. The vector [9, 7, 9, 19] is the structure in the real world, representing a network with 9, 7, 9, and 19 suppliers in each layer, respectively. The other two networks are synthetic, but they have similar scales. The results are shown in Figure 6.

C.6 Application: Package Delivery

For the case study of package delivery, our goal is to deliver packages to N residential areas. We want this path to be a Hamiltonian Path that visits each vertex (residential area) exactly once without necessarily forming a cycle. The goal is to determine whether such a path exists in a given graph.

Using an order-based formulation with variables $x_{i,j}$, where $x_{i,j}$ denotes that the i -th position

in the path is occupied by residential area j , i.e., residential area j is the i -th visited place.

$$x_{i,j} = \begin{cases} \text{True} & \text{if area } j \text{ is visited in the } i\text{-th position in the path,} \\ \text{False} & \text{otherwise.} \end{cases}$$

where the total number of variables is N^2 (for N cities).

To ensure that the variables $x_{i,j}$ correctly represent a valid Hamiltonian Path, several constraints must be enforced. These constraints formulate the Boolean satisfiability $\phi(x)$ in the SMC problem formulation.

- Each position is occupied by exactly one residential area. Or more formally, for every position i , exactly one residential area j must occupy it.

- At least one residential area per position:

$$\bigvee_{j=1}^n x_{i,j} \quad \forall i \in \{1, 2, \dots, n\}$$

- At most one residential area per position. For each position i and for every pair of distinct areas j and k :

$$\neg x_{i,j} \vee \neg x_{i,k} \quad \forall i \text{ and } \forall (j, k) \text{ such that } j < k$$

- Each residential area appears exactly once in the path. Each residential area j must be assigned to exactly one position i .

- At least one position per residential area.

$$\bigvee_{i=1}^n x_{i,j} \quad \forall j \in \{1, 2, \dots, n\}$$

- At most one position per residential area: For each area j and for every pair of distinct positions i and k :

$$\neg x_{i,j} \vee \neg x_{k,j} \quad \forall j \text{ and } \forall (i, k) \text{ such that } i < k$$

- Consecutive cities in the path are connected by an edge in the graph.

- For each pair of consecutive positions $(i, i + 1)$, the cities assigned must be connected by an edge. For all $i \in \{1, 2, \dots, n - 1\}$ and for all pairs of cities (j, k) not connected by an edge in the graph:

$$\neg x_{i,j} \vee \neg x_{i+1,k} \quad \forall (j, k) \notin E$$

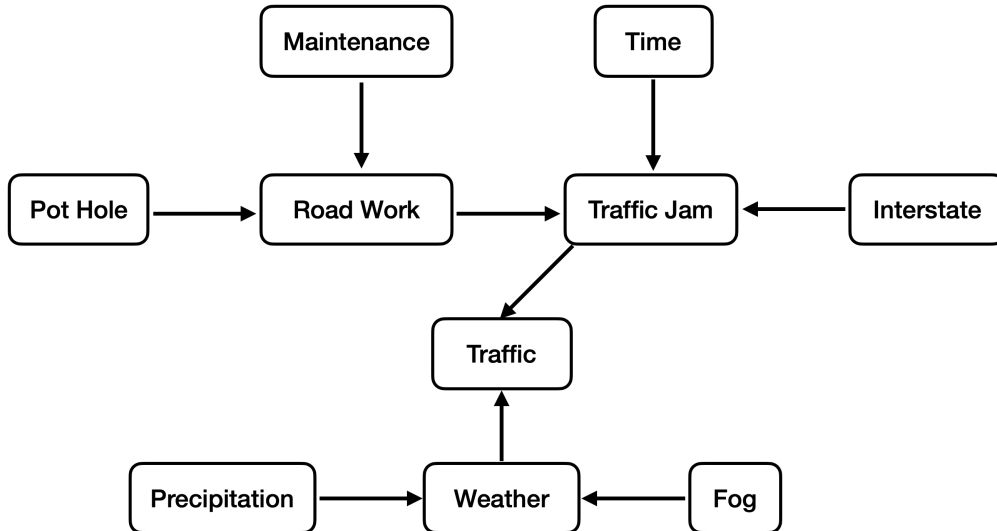


Figure 12: Bayesian network for a single road [20, 44].

Additionally, we want the schedule to have a very high probability ($\geq Q$) of encountering light traffic.

$$P(\text{light traffic}|\text{path}) = \sum_l P(\text{light traffic}, l|\text{path}) \geq Q$$

where l represents latent variables that affect the probability of traffic conditions, such as weather, road conditions, etc.

The graph structures used in our experiments are based on cropped regions from Google Maps (Figure 11). We consider three sets of delivery locations: 8 Amazon Lockers, 10 UPS Stores, and 6 USPS Stores. The three maps we examine are: Amazon Lockers only (Amazon), Amazon Lockers plus UPS Stores (UPS), and UPS graph with the addition of 6 USPS Stores (USPS). These graphs consist of 8, 18, and 24 nodes, respectively.

The traffic condition probability is modeled by the Bayesian network (Figure 12) from Los Angeles traffic data [44]. Instead of considering the “Time”, we use the order of traveling on a road to implicitly model the time.

To find the best route, we gradually decrease the threshold of the probability of encountering heavy traffic from 1 to 0 in increments of 10^{-2} , continuing until the threshold makes the SMC problem unsatisfiable. The running time for finding the best plan is shown in Figure 6 (Right).

D Additional Results

D.1 Knowledge Compilation Time

The time for compiling graphical models to decomposable deterministic and smooth probabilistic circuits is shown in Figure 13. As shown in the subsequent additional plots, the knowledge com-

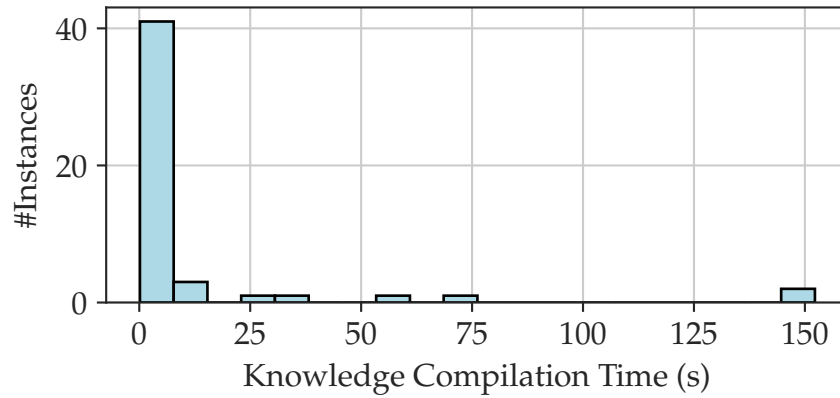


Figure 13: Histogram of the knowledge compilation time for all 50 probability distributions in the benchmark.

pilation time most significantly affects the running time of probabilistic models from DBN and Segmentation.

D.2 Comparison with Exact Solvers

Figure 3 (Left) is one illustrating example shown in the main text. Additional results on other SMCs consisting of different Boolean formulas and probabilistic graphical models are shown below.

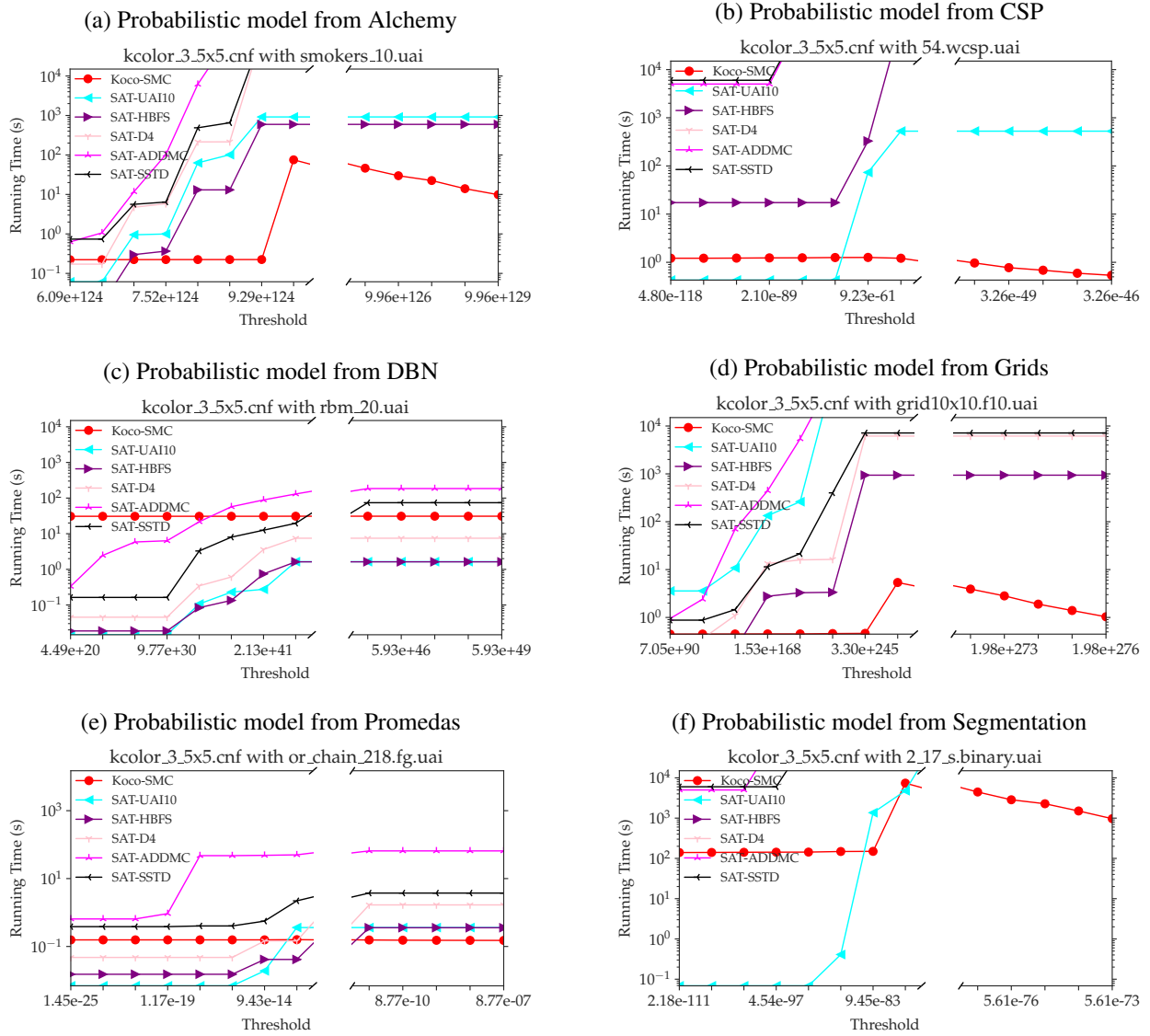


Figure 14: Results of SMC problems that consists of a fixed CNF file (*kcolor_3_5x5.cnf*) representing the 3 color problem on a 5×5 grid map and probabilistic graphical models from different categories.

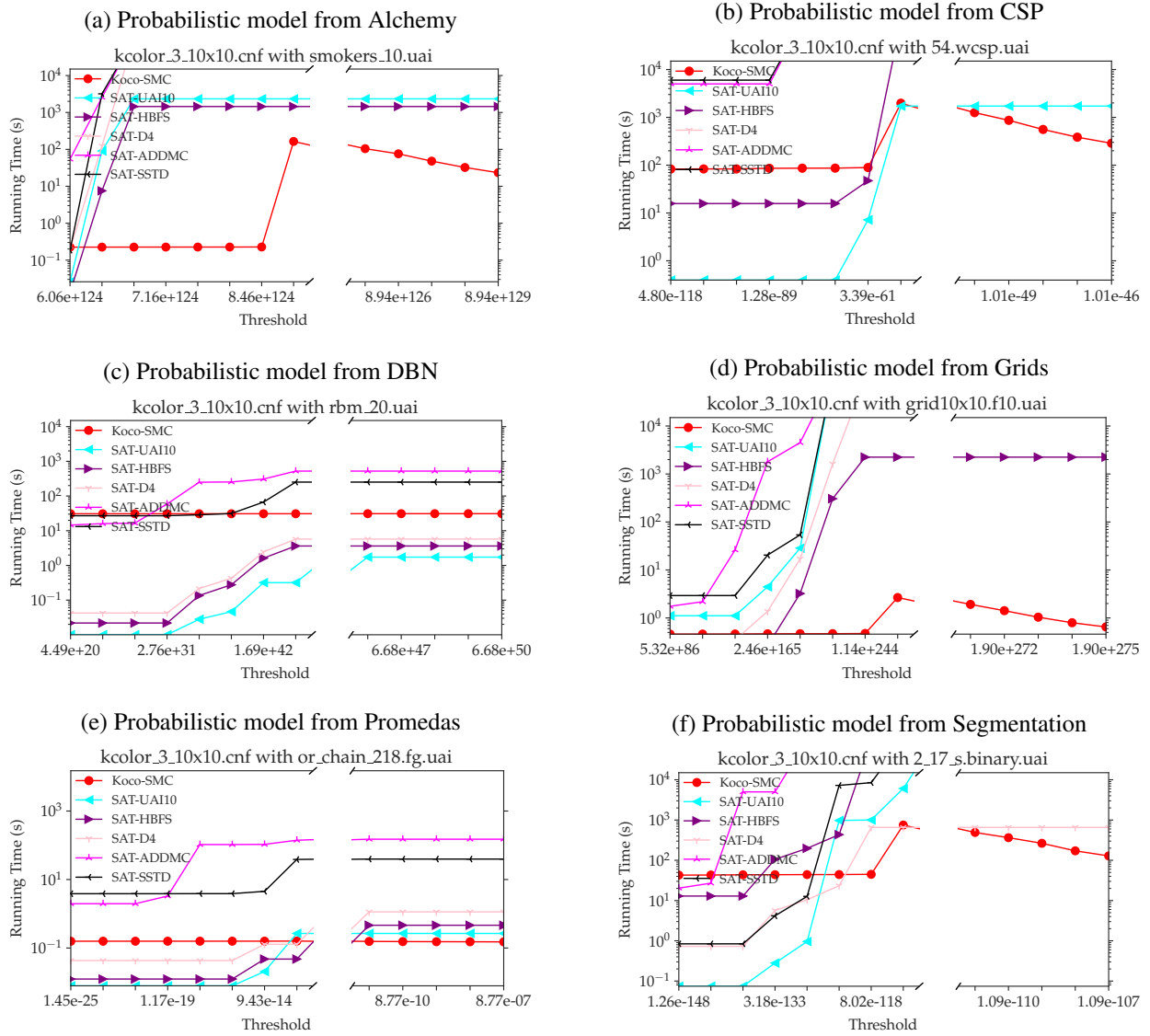


Figure 15: Results of SMC problems that consists of a fixed CNF file (*kcolor_3_10x10.cnf*) representing the 3 color problem on a 10×10 grid map and probabilistic graphical models from different categories.

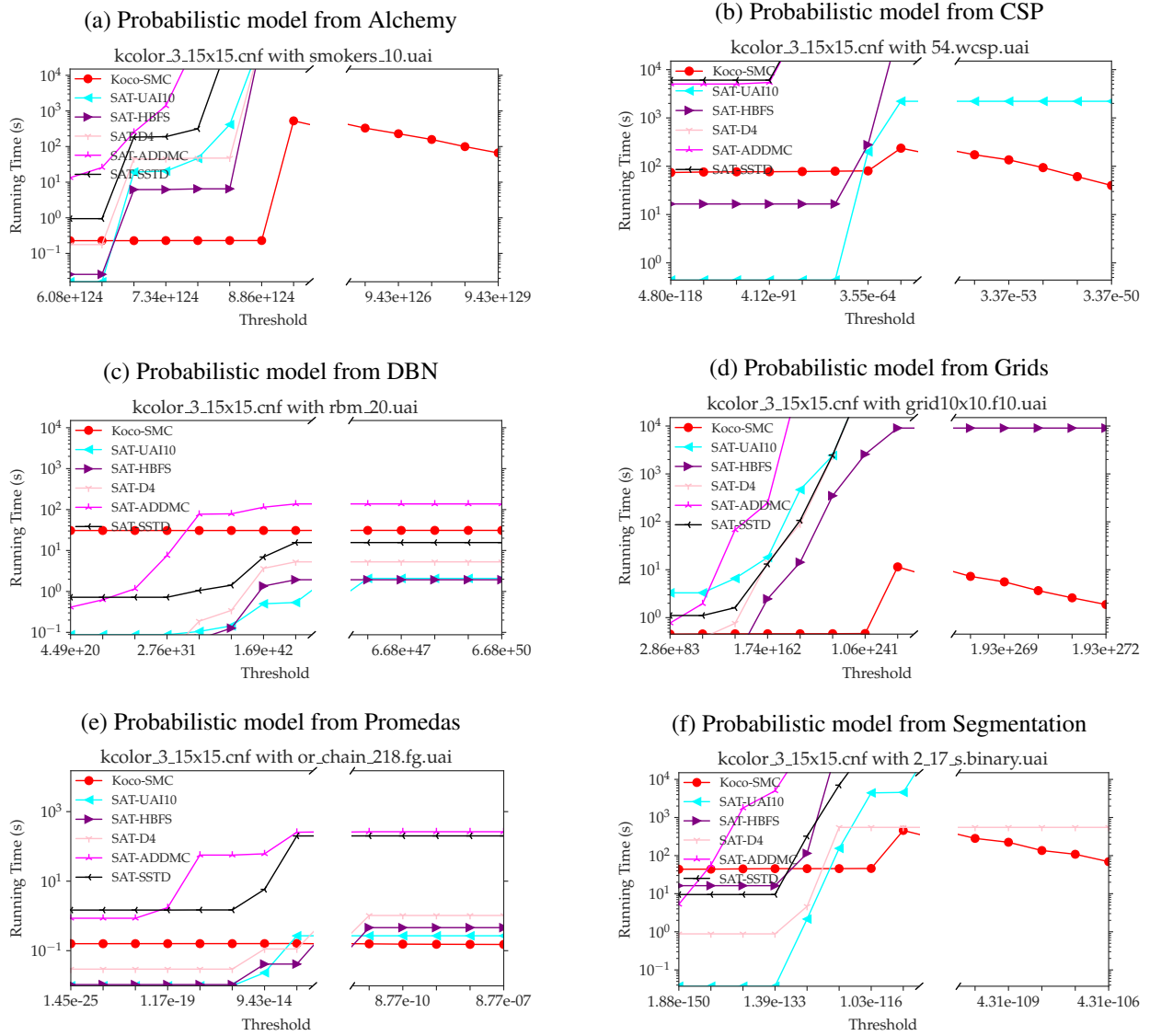


Figure 16: Results of SMC problems that consists of a fixed CNF file (*kcolor_3_15x15.cnf*) representing the 3 color problem on a 15×15 grid map and probabilistic graphical models from different categories.